

## Preparation of Transition Metal Orthophosphates, $MPO_4$ , and Their Magnetic Properties

NOBUKAZU KINOMURA\* AND FUMIO MUTO

*Institute of Inorganic Synthesis, Yamanashi University, 7 Miyamae-cho Kofu, 400, Japan*

AND MITSUE KOIZUMI

*Institute of Scientific and Industrial Research, Osaka University, Yamada-oka Suita, 565, Japan*

Received December 30, 1981; in revised form June 21, 1982

Transition metal orthophosphates with  $CrVO_4$ -type structure were prepared under various oxygen partial pressures. Lattice constants are  $a = 5.299$ ,  $b = 7.910$ , and  $c = 6.368$  Å for titanium phosphate and  $a = 5.230$ ,  $b = 7.772$ , and  $c = 6.284$  Å for  $VPO_4$ , respectively. The titanium phosphate was found to contain titanium vacancies. Magnetic susceptibility of  $VPO_4$  showed a broad maximum at about 140K because of its one-dimensional structure. The titanium phosphate had a nearly temperature-independent susceptibility over a wide temperature range. This suggests the existence of  $Ti^{3+}-Ti^{3+}$  homopolar bonds, but part of the bonds are broken by defects and subsequently isolated  $Ti^{3+}$  ions are produced in the structure. At low temperature,  $Ti^{4+}-\square-Ti^{4+}$  clusters would exist and cause a sharp decrease of the magnetic susceptibility. The temperature dependence of the EPR spectrum and magnetic susceptibility indicate gradual breakdown of  $Ti^{3+}-Ti^{3+}$  bonding.

### Introduction

Linkage of octahedra with sharing edges sometimes gives a short metal-metal distance, and the metal-metal bonding through shared edges has been observed in many compounds (1, 2). This strong interaction between metal ions causes interesting phenomena, such as metal-insulator transitions.  $Ti_nO_{2n-1}$  and  $V_nO_{2n-1}$ , known as Magnéli phases, are typical examples (3, 4). In these compounds,  $MO_6$  octahedra ( $M = Ti, V$ ) share corners and faces as well

as edges (5) and the second nearest cations are not far from a central cation.

The structure of  $CrVO_4$  is considered to be an intermediate structure between that of quartz and rutile from the viewpoint of phase transition under high pressures (6). In this structure, octahedra of  $CrO_6$  share only two edges at the opposite side with other octahedron and a one-dimensional chain of  $CrO_6$  octahedron is formed along the crystallographic  $c$  axis. The chains are combined by  $VO_4$  tetrahedron with sharing corners (7). Consequently, a chain of octahedron seen in the rutile structure is isolated from other chains.

Some orthophosphates with trivalent cations are isostructural with  $CrVO_4$  (8-10).

\* Inquiries and request for reprints should be made to this author.

By preparing titanium and vanadium orthophosphates with this structural type, one-dimensional chains composed of  $\text{TiO}_6$  and  $\text{VO}_6$  octahedra which are linked with edges could be isolated.

Here we report on the preparation and characterization of titanium and vanadium orthophosphate with  $\text{CrVO}_4$ -type structure.

### Experimental Procedure

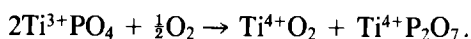
Powders of  $(\text{NH}_4)_2\text{HPO}_4$  and  $\text{TiO}_2$  (anatase) or  $\text{NH}_4\text{VO}_3$  were mixed in a molar ratio of 1.1 to 1.0 and were ground with an agate mortar and pestle. The mixtures were calcined at  $950^\circ\text{C}$  in a gold crucible under an atmosphere of Ar gas. In the case of vanadium phosphate, Ar gas was deoxidized by iron wire heated at  $550^\circ\text{C}$ . The  $P_{\text{O}_2}$  was estimated to be about  $10^{-26}$  atm from the diagram given by Swalin (11). A gold crucible containing starting powder for titanium phosphate was put at a sealed end of a silica tube whose other end was open, and porous titanium metal was packed into the remaining space of the silica tube. The silica tube was put in Ar gas and heated. The temperature at the titanium metal ranged between 950 and about  $750^\circ\text{C}$  along the packed column of titanium metal. In addition to the titanium metal, ammonium gas, which is produced by thermal decomposition of ammonium phosphate, reduces the oxygen partial pressure.

The compound  $\text{CrPO}_4$  was obtained by firing the precipitate, which was produced by mixing the solutions of  $\text{Cr}(\text{NO}_3)_3$  and  $(\text{NH}_4)_2\text{HPO}_4$  at  $1000^\circ\text{C}$  in air. The colors of the products were pale green for titanium phosphate, pale brown for vanadium phosphate, and green for  $\text{CrPO}_4$ .

Magnetic susceptibility was measured by using a Faraday balance from liquid He temperature to 600K. Electric resistance was measured on a polycrystalline sample sintered at  $900^\circ\text{C}$  and 3 GPa for 1 min using the two-probe method from room tempera-

ture to 600K. The measurement was carried out in He gas. The reproducibility was good in this temperature range, and samples were considered not to be oxidized during the measurement. Lattice constants were determined by least-squares refinement of powder data taken by using  $\text{Cu } K\alpha$  radiation with a scanning speed of  $\frac{1}{4}^\circ/\text{min}$ . EPR measurements on powder samples were performed from liquid  $\text{N}_2$  temperature to room temperature with a microwave frequency of 9.5 GHz. Spin concentration was measured by comparison with known samples of  $\text{CuSO}_4 \cdot 5\text{H}_2\text{O}$ .

Oxidation of the products was carried out at  $500^\circ\text{C}$  in  $\text{O}_2$  gas and the weight gain was measured until the weight gain remained at a constant value. The products upon oxidation were  $\text{VPO}_5$  for vanadium phosphate and almost amorphous white material with small and broad peaks of  $\text{TiO}_2$  and  $\text{TiP}_2\text{O}_7$  for titanium phosphate. The X-ray powder pattern of  $\text{VPO}_5$  produced from vanadium phosphate was sharp and extra peaks were not observed. The calculated values for the weight gain were based on the following reactions.



These values correspond to the weight changes accompanied with the oxidation of  $\text{V}^{3+}$  or  $\text{Ti}^{3+}$  to their highest oxidation states, being independent on the crystalline state of the products.

The ratio of Ti/P was determined with the gravimetric analysis to be 0.965.

### Result

X-Ray powder patterns for titanium phosphate and vanadium phosphate were similar to that of  $\beta\text{-CrPO}_4$  and were completely indexed with orthorhombic unit cells. The X-ray powder pattern of chromium phosphate agreed with the reported

one for  $\beta$ -CrPO<sub>4</sub> (10). The lattice constants and weight gain with oxidation for titanium phosphate and vanadium phosphate are listed in Table I. In Fig. 1, lattice constants of phosphates with CrVO<sub>4</sub>-type structure are plotted against ionic radii of transition metal ions. As seen in this figure, the lattice constants increase linearly with an increase of ionic radii. In this series of compounds, a discontinuity of lattice constants was not observed, although such phenomena were reported for the *c* axis of transition metal dioxides with rutile-type structure (12). The metal-metal bonding through shared edges is associated with the sharp decrease of the *c* axis in these compounds.

The single phase of vanadium phosphate with CrVO<sub>4</sub>-type structure changed to the single phase of VPO<sub>5</sub> with oxidation and the weight gain upon oxidation was 11.0%, in good agreement with the calculated value. This indicates that the compound obtained is almost stoichiometric VPO<sub>4</sub>. On the other hand, the weight gain upon oxidation for titanium phosphate was smaller than the calculated value, which is based on the stoichiometric TiPO<sub>4</sub>. The chemical analysis showed the deviation of molar ratio of Ti/P from unity.

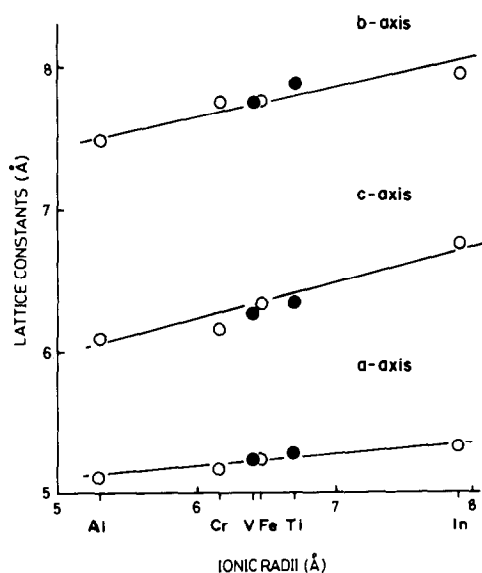


FIG. 1. Lattice constants vs ionic radii for  $M^{3+}$ PO<sub>4</sub> orthophosphates.

The chemical formula for the titanium phosphate should be given as  $Ti_{1-x}^{3+}Ti_{3x}^{4+}\square_xPO_4$ , where  $\square$  is a titanium vacancy. One cation vacancy introduced into the structure results in producing three trivalent titanium ions for the charge compensation. The value of *x* is determined to be 0.035 from the chemical analysis, and

TABLE I

LATTICE CONSTANTS AND WEIGHT GAIN WITH OXIDATION OF TRANSITION METAL ORTHOPHOSPHATES AND CRITICAL DISTANCE FOR METAL-METAL BONDING

	<i>a</i> (Å)	<i>b</i> (Å)	<i>c</i> (Å)	Critical distance <sup>a</sup> (Å)	Weight gain (%)	
					Obs.	Calc.
TiPO <sub>4</sub> <sup>b</sup>	5.299	7.910	6.368	3.02	4.8	5.5
VPO <sub>4</sub> <sup>c</sup>	5.230	7.772	6.284	2.94	11.0	11.0
$\beta$ -CrPO <sub>4</sub> <sup>d</sup>	5.165	7.750	6.131	2.84		
FePO <sub>4</sub> <sup>e</sup>	5.277	7.770	6.322	2.58		

<sup>a</sup> Ref. (16).

<sup>b</sup> This work. This formula is given here for the simplicity in spite of its nonstoichiometry. See text.

<sup>c</sup> This work.

<sup>d</sup> Ref. (10).

<sup>e</sup> Ref. (9).

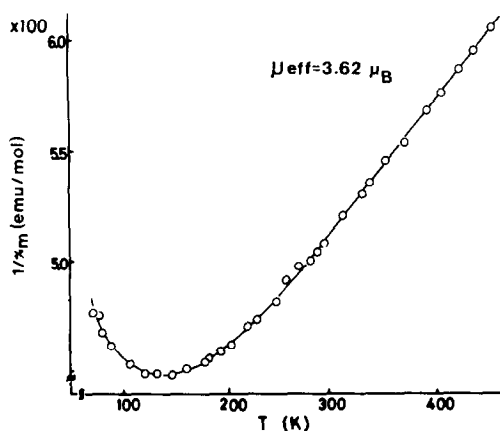


FIG. 2. Magnetic susceptibility vs temperature for  $VPO_4$ .

the chemical formula for the titanium phosphate obtained here is deduced to be  $Ti_{0.860}^{3+}Ti_{0.105}^{4+}\square_{0.035}PO_4$ . The value of  $x$  probably depends on the oxygen partial pressure, although we have not studied this.

The temperature dependence of magnetic susceptibility for  $VPO_4$  is shown in Fig. 2. A broad minimum was observed for  $1/\chi$  at about 140K and the effective magnetic moment was calculated to be  $3.6\mu_B$  in the high-temperature region. The broad minimum of  $1/\chi$  may reflect the one-dimensional structure of this compound. The magnetic susceptibility for  $CrPO_4$  seems to obey the Curie-Weiss law (Fig. 3). No ordering temperature was observed down to liquid  $N_2$  temperature and the observed effective magnetic moment of  $3.9\mu_B$  is in good agreement with the spin-only value for  $Cr^{3+}$ . The paramagnetic Curie temperature was calculated to be  $-529K$  for  $VPO_4$  and  $-80K$  for  $CrPO_4$ , respectively.

As shown in Fig. 4, the magnetic susceptibility of titanium phosphate is nearly independent of temperature above about 140K. Below this temperature, the magnetic susceptibility decreased to about half that at high temperature, and then increased again on going to liquid He temperature. In this temperature region, the data were fitted by

the law

$$x_g = x_0 + (C_g/(T - \theta)),$$

where  $x_0$  was a temperature-independent contribution. The constants were determined to be  $2.1 \times 10^{-7}$  emu/g for  $x_0$ ,  $51.5 \times 10^{-6}$  emu/g for  $C_g$ , and  $-1.5K$  for  $\theta$ , respectively.

From the measurement of electrical resistance, the titanium phosphate is considered to be a semiconductor with an activation energy of 0.67 eV as seen in Fig. 5. The electrical resistance of  $VPO_4$  is also shown in Fig. 5. This compound is a semiconductor with an activation energy of 1.14 eV. The electrical resistance below room temperature was not measured because of their high values.

An EPR spectrum for the titanium phosphate at 292K is shown in Fig. 6. The peculiar magnetic behavior and the magnitude of magnetic susceptibility of the titanium phosphate imply that the  $Ti^{3+}-Ti^{3+}$  homopolar bond exists in this compound. However, the fairly strong spectrum observed indicates that a considerable amount of unpaired  $Ti^{3+}$  also exists. We think that the unpaired  $Ti^{3+}$  ions are caused by the nonstoichiometry of this compound, as observed for  $Ti_4O_7$  (13, 14). The  $g$  factor of this compound was 1.940 and is smaller than those reported for  $Ti_nO_{2n-1}$  (15). The

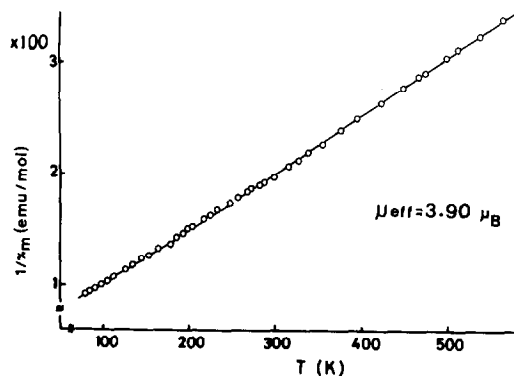


FIG. 3. Magnetic susceptibility vs temperature for  $CrPO_4$ .

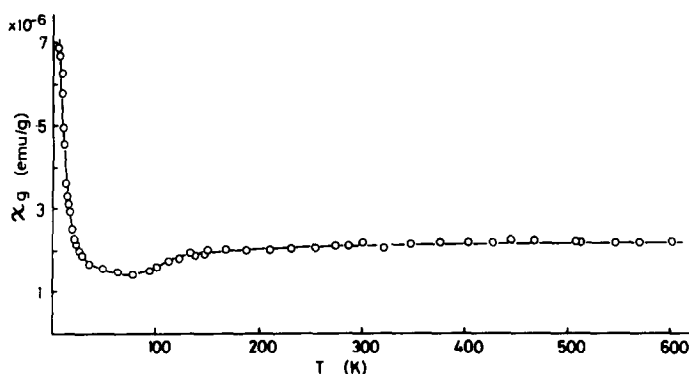


FIG. 4. Magnetic susceptibility vs temperature for titanium phosphate.

intensity of the spectrum remained nearly constant down to about 150K, and this indicates that the spin concentration declines with a decrease in temperature. In Fig. 7, the temperature dependence of spin concentration and linewidth are shown. At the temperature region where magnetic susceptibility decreases, the spin concentration also decreases sharply and the linewidth continues to become narrow. These facts suggest that the sharp decrease in magnetic susceptibility is not associated with the magnetic ordering.

## Discussion

In Table I, lattice constants of the transi-

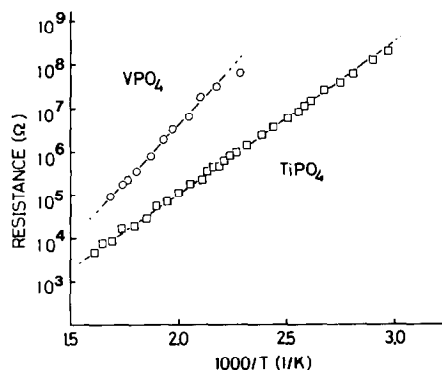


FIG. 5. Electric resistance of  $VPO_4$  and titanium phosphate at elevated temperature.  $\square$ : titanium phosphate,  $\circ$ :  $VPO_4$ .

tion metal phosphates,  $MPO_4$ , are listed, as well as the critical distance for metal-metal bonding proposed by Goodenough (16). The half-length of the  $c$  axis of the  $CrVO_4$ -type structure gives the metal-metal bond length through a shared edge. The phosphates listed here have larger values than the critical distances of the corresponding ions. We cannot, therefore, expect metal-metal bonding for these compounds. The data for  $VPO_4$ ,  $CrPO_4$ , and  $FePO_4$  support this model.

Although no magnetic ordering was observed, the magnetic susceptibility of the titanium phosphate is almost temperature independent above 140K and its magnitude is smaller than the expected value for free  $Ti^{3+}$  ion. This fact indicates the existence of  $Ti^{3+}-Ti^{3+}$  homopolar bonds. Short Ti-Ti distances for paired  $Ti^{3+}$  would alternate

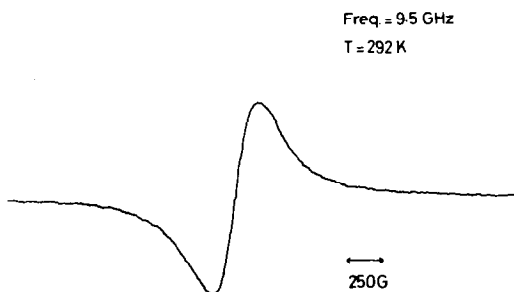


FIG. 6. EPR spectrum of polycrystalline titanium phosphate.

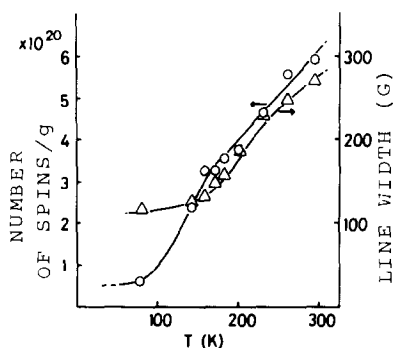


FIG. 7. EPR spin concentration and linewidth vs temperature for titanium phosphate.  $\circ$ : spin concentration;  $\triangle$ : linewidth.

with long Ti-Ti distances for nonbonded  $Ti^{3+}$  along the chain but the distribution of the pairs would be random in the structure. Since the  $c$  axis length gives only the average distance of paired and unpaired  $Ti^{3+}$  ions in this case, no extraordinary change of lattice constants with the ionic radius of constituent transition metal ions was observed.

The defects (titanium vacancies and  $Ti^{4+}$  ions) inhibit the formation of  $Ti^{3+}-Ti^{3+}$  pairs and leave unpaired  $Ti^{3+}$  ions which contribute to the EPR. The concentration of unpaired  $Ti^{3+}$  depends strongly on the number of defects. At high temperatures, the defects would distribute randomly in the chain and one defect has at least one unpaired  $Ti^{3+}$  ion as its neighbor when one of the paired  $Ti^{3+}$  ions is replaced with a defect. In this case, the concentration of unpaired  $Ti^{3+}$  is calculated to be 14.0%, in good agreement with the observed value of 14% at 292K by EPR. But, it is not necessary that the concentration of unpaired  $Ti^{3+}$  corresponds exactly to the number of defects, because unpaired  $Ti^{3+}$  ions produced by the replacement of the counterpart of a pair with a defect, as mentioned above, would tend to recombine with other isolated  $Ti^{3+}$  ions for the stabilization of the compound, especially at low temperatures. The number of defects gives the maximum

concentration of isolated  $Ti^{3+}$  ions in this case.

Cation vacancy and  $Ti^{4+}$  ions may tend to form clusters shown as  $Ti^{4+}-\square$  and  $Ti^{4+}-\square-Ti^{4+}$  with a decrease in temperature. The last form of cluster is most likely at very low temperature, as reported for  $Fe_{1-x}O$  (17). If the final state of defects is a combination of the cluster  $Ti^{4+}-\square-Ti^{4+}$  and isolated  $Ti^{4+}$ , the number of defects decreases to half of random distribution of defects at high temperatures. As the number of defects decreases, the unpaired  $Ti^{3+}$  ions which were accompanied with the defects are released from the defects and pair with other released  $Ti^{3+}$  ions. Therefore the clustering diminishes the population of unpaired  $Ti^{3+}$  ions. The magnitude of the magnetic susceptibility and spin concentration should decrease in accordance with the clustering of defects and the decrease of unpaired  $Ti^{3+}$  ions. In fact, both the magnetic susceptibility and spin concentration decreased abruptly below 150K as shown in Figs. 4 and 7. We think the formation of  $Ti^{4+}-\square-Ti^{4+}$  clusters is mainly responsible for these abrupt decreases.

The concentration of unpaired  $Ti^{3+}$  ions is considered to remain constant below about 100K, because a rearrangement of defects is no longer expected. In fact, the magnetic susceptibility exhibited a Curie-Weiss behavior as shown in Fig. 4 and the Curie constant was calculated to be  $52 \times 10^{-6}$  emu/g. Taking the spin concentration of  $0.60 \times 10^{20}$  spins/g, which was observed at 77K, we can calculate an effective magnetic moment of  $2.0\mu_B$  for the temperature region below 100K. This value shows a good agreement with the spin-only moment of  $1.7\mu_B$  for  $Ti^{3+}$ .

In addition to the clustering of defects, the breakdown of  $Ti^{3+}-Ti^{3+}$  pairs must be taken into account in order to explain the nearly temperature-independent magnetic susceptibility above 150K. Up to room temperature, the spin concentration was ob-

served to increase with temperature. EPR spectra were not measured above room temperature, but temperature-independent susceptibility above room temperature indicated that isolated  $Ti^{3+}$  ions continue to increase with temperature. The amount of isolated  $Ti^{3+}$  ions estimated from the magnetic susceptibility was more than that calculated on the assumption that a defect accompanies an isolated  $Ti^{3+}$  ion as a result of substitution of the counterpart of a  $Ti^{3+}-Ti^{3+}$  pair by a defect. This means that a gradual breakdown of  $Ti^{3+}-Ti^{3+}$  pairs takes place.

In the Magnéli-phase series of compounds, breakdown of pairs occurs at a critical temperature and accompanies the metal-insulator transition. However, this is not the case for titanium phosphate. Electric resistance and magnetic susceptibility do not exhibit such a critical transition but the  $Ti^{3+}-Ti^{3+}$  bonding is broken gradually. Fairly large concentration of defects may strongly affect the gradual breakdown of  $Ti^{3+}-Ti^{3+}$  bonding.

## References

1. J. B. GOODENOUGH, *J. Appl. Phys.* **31**, 359 (1960).
2. F. A. COTTON, *Quart. Rev. (London)* **20**, 389 (1966).
3. J. F. HOULIHAN, W. J. DANLEY, AND L. N. MULAY, *J. Solid State Chem.* **12**, 265 (1975).
4. A. C. GOSSARD, J. P. REMEIK, T. M. RICE, H. YASUOKA, K. KOSUGE, AND S. KACHI, *Phys. Rev. B* **9**, 1230 (1974).
5. A. F. WELLS, "Structural Inorganic Chemistry," 4th ed., Chap. 12, Oxford Univ. Press (Clarendon), London/New York (1975).
6. O. MULLER AND R. ROY, "The Major Ternary Structure Families," Chap. 3 (Crystal Chemistry of Non-Metallic Materials Series, Vol. 4, Springer-Verlag, Berlin/Heidelberg/New York (1974).
7. K. BRANDT, *Ark. Kemi. Mineral. Geol. A* **17**, 1 (1943).
8. K. H. SEIFERT, *Fortschr. Mineral.* **45**, 214 (1968).
9. N. KINOMURA, M. SHIMADA, M. KOIZUMI, AND S. KUME, *Mater. Res. Bull.* **11**, 457 (1976).
10. *Nat. Bur. Standard Cir.* 539, **9**, 26 (1959).
11. R. A. SWALIN, "Thermodynamics of Solids," Chap. 7, Wiley, New York (1962).
12. D. B. ROGERS, R. D. SHANNON, A. W. SLEIGHT, AND J. L. GILLSON, *Inorg. Chem.* **8**, 841 (1969).
13. S. LAKKIS, C. SCHLENKER, B. K. CHAKRAVERTY, R. BUDER, AND M. MAREZIO, *Phys. Rev. B* **14**, 1429 (1976).
14. J. F. HOULIHAN AND L. N. MULAY, *Phys. Status Solidi B* **61**, 647 (1974).
15. J. F. HOULIHAN AND L. N. MULAY, *Inorg. Chem.*, **13**, 745 (1974).
16. J. B. GOODENOUGH, "Metallic Oxides," in "Progress in Solid State Chemistry" (H. Reiss, Ed.), Vol. 5, Pergamon, New York (1971).
17. R. COLLONGUES, Thesis No. 3805, Paris (1954).